

Photoneutron Cross Sections of Ta¹⁸¹ and Ho¹⁶⁵

R. L. BRAMBLETT, J. T. CALDWELL, G. F. AUCHAMPAUGH, AND S. C. FULTZ
Lawrence Radiation Laboratory, University of California, Livermore, California

(Received 29 October 1962)

The (γ, n) and $(\gamma, 2n)$ cross sections for Ta¹⁸¹ and Ho¹⁶⁵ have been measured by use of nearly monochromatic photons obtained from the annihilation-in-flight of fast positrons. The integrated cross sections up to 28 MeV for $\sigma(\gamma, n)$ and $\sigma(\gamma, 2n)$, respectively, are 1.32 ± 0.13 and 0.93 ± 0.09 MeV-b for Ta, and 1.47 ± 0.15 and 0.90 ± 0.09 MeV-b for Ho. Values obtained for σ_{-2} are 10.88 and 10.93 mb/MeV, respectively, for these elements. The level density parameters, a , were determined to be 15.7 and 22.0 reciprocal MeV, respectively. The intrinsic quadrupole moments determined from the compound nucleus formation cross sections, were found to be 6.71 ± 0.74 and 7.40 ± 0.90 b for Ta and Ho, respectively.

INTRODUCTION

EARLY studies on highly deformed nuclei were undertaken by means of Coulomb excitation. For many such nuclei the energies, spins, and parities of the lowest excited rotational states along with quadrupole transition probabilities $BE2$, have been measured. From this information the intrinsic quadrupole moments, Q_0 , of nuclei may be obtained.¹

More recently, Danos² and Okamoto³ have shown that the giant dipole resonances for highly deformed spheroidal nuclei should be resolvable into two characteristic resonances. The ratio of the energies at which the peak cross sections for these resonances occur is simply related to the quadrupole moment of the nucleus. A number of nuclei have been examined at other laboratories to establish the presence of structure in the giant dipole resonance. In all cases the data were obtained by the use of continuous bremsstrahlung radiations and, therefore, contain features characteristic of this method. For such a method, the cross section is obtained by unfolding the bremsstrahlung spectra from activation or neutron yield curves. Analysis in the region above the peak of the giant resonance yields large intrinsic errors, since it involves small differences between large numbers. Another factor which affects the reliability of the earlier measurements includes the uncertainty in the estimates given for the contribution to the photoneutron cross section arising from the higher multiplicity $(\gamma, 2n)$ reactions. This was usually calculated from roughly estimated values for the level density parameter, and was therefore subject to large errors. The above factors seriously affected the accuracy with which the shape of the giant resonance was determined on the high-energy side, a region very important to analysis of the giant resonance and the determination of nuclear shape parameters. An additional factor which affected the determination of the latter was the manner of selection of the parameters which determine the component Lorentz lines in the giant resonance. In general, these were arbitrarily selected in order that a reasonable fit to the data be obtained.

The measurements and analysis described in this report were obtained by use of methods designed to attempt to overcome some of the shortcomings of those previously employed. Essentially monochromatic photons were used, so that no unfolding procedure was required to obtain the cross-section dependence on photon energy. The contributions to the cross section arising from higher multiplicity reactions were measured, and the level density parameters were directly determined. A method was developed for fitting Lorentz lines to the photoneutron giant resonance whereby arbitrariness in the choice of values for the Lorentz line parameters is much reduced.

APPARATUS AND PROCEDURE

The measurements on the photoneutron cross sections for Ta¹⁸¹ and Ho¹⁶⁵ described herein were made by the use of nearly monochromatic photons obtained from the annihilation-in-flight of fast positrons.^{4,5} The positrons were created by pair production from 10-MeV bremsstrahlung, at the center of a two-stage linear electron accelerator, and were accelerated in the second section to the desired energy. They were then energy-analyzed by use of a beam bending magnet, and made to pass through a thin target of Be or LiH. On passing through this "annihilation" target, some of the positrons annihilate in flight with electrons in the target material through the two-photon annihilation process. The annihilation photons created in the forward direction had energies about 0.76 MeV greater than the energies of the positrons, and their energy resolution was approximately 3%.⁶ The photons were measured by means of a transmission ion chamber filled with xenon to a pressure of 1 atm. The ion chamber was calibrated by use of a NaI(Tl) gamma-ray spectrometer having a 6-in.-long \times 5-in.-diam crystal. The neutrons emitted by the sample were detected in a 4II paraffin-moderated neutron detector.

The photoneutron samples usually consisted of several disks of metal rigidly mounted in a container con-

¹ K. Alder, A. Bohr, T. Huus, B. Mottleson, and A. Winther, *Rev. Mod. Phys.* **28**, 432 (1956).

² M. Danos, *Nucl. Phys.* **5**, 23 (1956).

³ K. Okamoto, *Progr. Theoret. Phys. Japan* **15**, 75 (1956).

⁴ S. C. Fultz, R. L. Bramblett, J. T. Caldwell, and N. A. Kerr, *Phys. Rev.* **127**, 1273 (1962).

⁵ S. C. Fultz, R. L. Bramblett, J. T. Caldwell, N. E. Hansen, and C. P. Jupiter, *Phys. Rev.* **128**, 2345 (1962).

⁶ C. R. Hatcher, R. L. Bramblett, N. E. Hansen, and S. C. Fultz, *Nucl. Instr. Methods* **14**, 337 (1961).

structed of plastic foam. Powdered samples were placed in thin plastic containers. The neutron yield and the number of photons incident on the sample were simultaneously measured for a number of selected positron energies ranging from 8.5 to 28 MeV. The magnetic fields were then reversed and the negative halves of the pairs were selected in order to obtain a beam of negative electrons of similar intensity to that of the positrons. For each selected energy of negative electrons, simultaneous measurements were made of the number of neutrons and photons, until a range of energies corresponding to those examined with the positrons had been covered. The fraction of photon neutrons arising from the positron bremsstrahlung was easily deduced from these measurements, and was subtracted from the neutron data.

The neutron counts were electronically separated as single, double, or triple counts occurring during the gating interval (335 μ sec) per beam pulse. The counts recorded per beam pulse were statistically correlated to the number of neutrons emitted per nuclear disintegration. From this the (γ, n) and $(\gamma, 2n)$ cross sections were deduced. More details of the experimental procedure may be found in previous reports.^{4,5}

PHOTON MEASUREMENTS

The Xe-filled transmission ion chamber was used to measure the absolute number of annihilation photons incident on the photon neutron sample. The ion chamber was usually calibrated by measuring the charge collected from it simultaneously with the number of annihilation photons. The latter were measured by use of the gamma-ray spectrometer. For this process, it is necessary to calculate the detection efficiency of the NaI(Tl) crystal, (which involves a knowledge of the absorption coefficients) and to know the shapes of the crystal response functions for monochromatic gamma rays of various energies. The data used for these calculations were obtained from sources which utilized both experimental and computational methods.^{7,8}

An additional experiment was undertaken in order to obtain an independent confirmation of the spectrometer method for measuring the number of annihilation gamma rays. For this, the ion chamber was calibrated through its response to the number of annihilation photons entering it, as calculated from the positron current incident upon a thin (0.005 in.) Be annihilation target. The positron current was measured by periodic sampling of the beam by use of a Faraday cup which could be remotely operated. At the same time, an ion chamber calibration was undertaken in the usual manner, using the gamma-ray spectrometer. The number of annihilation photons created in the Be target, which were emitted within the solid angle subtended by the ion chamber, were calculated from the measured posi-

tron current and the differential annihilation cross section.⁹ The effect of multiple scattering of the positrons within the Be target was calculated by use of the multiple scattering theory of Molière.¹⁰ If $N(\theta, x)$ denotes the angular distribution of positrons at a depth x , and the macroscopic differential annihilation cross section is $\Sigma(\theta)$, the number of annihilation photons per positron per steradian at 0° to the incident beam is

$$A = 2\pi \int_{\theta=0}^{\pi} \int_{x=0}^t \Sigma(\theta) \tan\theta N(\theta, x) d\theta dx, \quad (1)$$

where θ defines the direction of the annihilating positron after scattering, and t is the thickness of the target.

The ion chamber response per annihilation photon was obtained by using the response per positron and Eq. (1). In Table I the results are compared with the calibration obtained by analysis of the gamma spectrometer data. The ratio of the number of annihilation photons measured by use of the gamma spectrometer to that calculated from the differential annihilation cross section, ranged from 0.91 ± 0.06 to 1.16 ± 0.12 . The average value for the ratio was 0.98 with an average deviation of 3%. The two methods of photon measurement, therefore, are in close agreement.

EXPERIMENTAL RESULTS

A. Tantalum

Photon neutron cross-section measurements on Ta¹⁸¹ have previously been made by a number of investigators.¹¹⁻²¹ A summary of some of the results obtained are

TABLE I. Ratio of the number of annihilation photons measured by use of a gamma-ray spectrometer to those deduced from measurement of the number of positrons.

Annihilation photon energy (MeV)	Ratio of annihilation photons
9.39	1.05 \pm 0.07
10.31	1.16 \pm 0.12
15.57	0.91 \pm 0.06
18.66	1.01 \pm 0.06
23.30	0.91 \pm 0.06
Mean	0.977 \pm 0.031

⁹ W. Heitler, *The Quantum Theory of Radiation* (Oxford University Press, New York, 1954), 3rd ed.

¹⁰ G. Molière, *Z. Naturforsch* **34**, 78 (1948).

¹¹ R. Nathans and J. Halpern, *Phys. Rev.* **93**, 437 (1954).

¹² J. Goldemberg and L. Katz, *Can. J. Phys.* **32**, 49 (1954).

¹³ B. I. Gavrilov and L. E. Lazareva, *Soviet Phys.—JETP* **3**, 871 (1957).

¹⁴ $\sigma_{-2} = \int_0^\pi \sigma dE/E^2$ defines the "second moment" or "minus second" cross section as discussed by J. S. Levinger, in *Nuclear Photodisintegration* (Oxford University Press, New York, 1960).

¹⁵ J. H. Carver and W. Turchinets, *Proc. Phys. Soc. (London)* **71**, 613 (1958).

¹⁶ E. G. Fuller and M. S. Weiss, *Phys. Rev.* **112**, 560 (1958).

¹⁷ R. W. Parsons and L. Katz, *Can. J. Phys.* **37**, 809 (1959).

¹⁸ B. M. Spicer, H. H. Thies, J. E. Baglin, and F. R. Allum, *Australian J. Phys.* **11**, 298 (1958).

¹⁹ J. Miller, C. Schuhl, and C. Tzara, *Nucl. Phys.* **32**, 236 (1962).

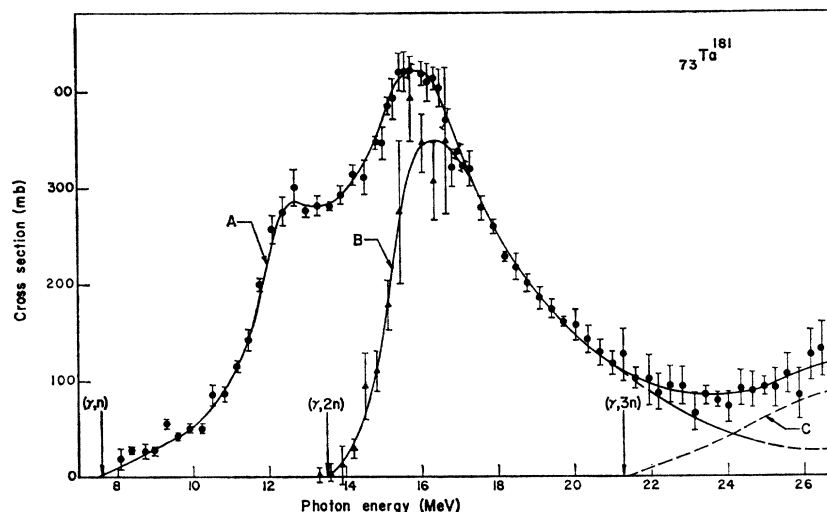
²⁰ W. H. Hartley, W. E. Stephens, and E. J. Winhold, *Phys. Rev.* **104**, 178 (1956).

²¹ R. E. Welsh and D. J. Donahue, *Phys. Rev.* **121**, 880 (1961).

⁷ G. W. Grodstein, National Bureau of Standards Circular No. 583 (U. S. Government Printing Office, Washington, D. C., 1957).

⁸ J. Kockum and N. Starfelt, *Nucl. Instr. Methods* **4**, 171 (1959).

FIG. 1. Cross sections for Ta from neutron yield data. Curve A consists of $\sigma(\gamma, n) + 2\sigma(\gamma, 2n) + \sigma(\gamma, np) + 3\sigma(\gamma, 3n)$ and was obtained from single-neutron counting data. Curve B contains $2\sigma(\gamma, 2n)$ and was obtained from double-neutron counting data. Curve C contains the estimated contribution of $3\sigma(\gamma, 3n)$ to the singles data.



given in Table II. Gavrilov and Lazareva⁸ obtained for σ_{-2} ¹⁴ the value of 13.9 mb/MeV. Carver and Turchinets¹⁵ obtained an integrated cross section up to 31 MeV of 3.3 ± 1.2 MeV-b. The relative contributions for (γ, n) , $(\gamma, 2n)$, and $(\gamma, 3n)$ reactions were determined by the foil activation method and were found to be 73 ± 3 , 24 ± 2 , and $3.0 \pm 1.2\%$, respectively. Fuller and Weiss¹⁶ observed evidence of splitting in the giant resonance for Ta. Similar observations on splitting were made by Parsons and Katz¹⁷ and by Spicer and co-workers.¹⁸ Data on the components of the giant resonances, where splitting was observed, are shown in the fourth, fifth, and sixth lines of Table II. Integrated cross sections corrected for neutron multiplicity are given in references 15 to 18 inclusive. Miller, Schuhl, and Tzara¹⁹ recently measured the photoneutron cross section for Ta using annihilation photons. Their data show peaks in the total cross-section curve as shown in Table II. Hartley and Stephens²⁰ obtained 420 and 320 mb for the total photoneutron cross sections at 14.8 and 17.6 MeV, respectively, on using Li(p, γ) gamma rays. Welsh and Donahue²¹ measured these cross sections at several gamma-ray energies using capture gamma rays from various source materials.

The data obtained from the present measurements are shown in Fig. 1. The excitation function for the total

neutron yield $\sigma(\gamma, n) + \sigma(\gamma, np) + 2\sigma(\gamma, 2n) + 3\sigma(\gamma, 3n)$ (top curve) has two peaks; one at 12.70 MeV (approximately 285 mb) and the other at 15.5 MeV (approximately 420 mb). The lower curve was obtained from the double neutron counts and represents $2\sigma(\gamma, 2n)$. The $(\gamma, 3n)$ threshold calculated from mass data,²² occurs at 21.3 MeV. A slight contribution from the $(\gamma, 3n)$ reaction is apparent on the high-energy portion of the total yield curve. The dashed curve is a rough estimate of $3\sigma(\gamma, 3n)$, based upon a few triple neutron counts. The top and lower curves blend together above 17 MeV, within the errors of measurement. For clarity of presentation, the data from the double neutron counting have been omitted above 17 MeV, although they are shown in Fig. 2. The measured threshold for the $(\gamma, 2n)$ reaction is 13.6 ± 0.2 MeV. This compares favorably with the value 13.64 MeV calculated from mass data.²² The (γ, n) and $(\gamma, 2n)$ cross sections are shown in Fig. 2. The $\sigma(\gamma, n)$ curve has a peak cross section of approximately 280 mb at 13.5 MeV, while the $(\gamma, 2n)$ cross section curve has a peak of 170 mb at 16.5 MeV. The integrated cross sections up to 28 MeV, for the (γ, n) and $(\gamma, 2n)$ curves are: 1.32 ± 0.13 and 0.93 ± 0.09 MeV-b, respectively. The formation cross section for the compound nucleus of Ta¹⁸¹ was obtained from the sum of the data from the $\sigma(\gamma, n)$ and $\sigma(\gamma, 2n)$ curves, and is given in Fig. 3. The solid curve is the sum of two Lorentz lines. The width at half-maximum is 6.4 MeV and the integrated cross section is 2.21 ± 0.22 MeV.

B. Holmium

The photoneutron cross section for Ho¹⁶⁵ was measured by Fuller, Petree, and Weiss²³ using a betatron and the neutron counting method. They obtained a

²² V. J. Ashby and H. C. Catron, University of California Radiation Laboratory Report UCRL-5419, 1959 (unpublished).

²³ E. G. Fuller, B. Petree, and M. S. Weiss, Phys. Rev. 112, 554 (1958).

TABLE II. Photoneutron data on the Ta giant resonance. The symbols σ_1 , σ_2 , E_1 , E_2 , and Γ_1 , Γ_2 denote the peak cross sections, energies at which the maxima in the cross sections occur, and widths at half-maximum of component Lorentz lines where fitted.

σ_1 (mb)	σ_2 (mb)	E_1 (MeV)	E_2 (MeV)	Γ_1 (MeV)	Γ_2 (MeV)	$\int \sigma dE$	reference No.
397		15.1		7.9		3.43	11
630		15.0		6.0		4.1	12
452		14.5		6.8		3.87	13
308	348	12.45	15.45	2.3	4.4	3.39	16
317	444	12.5	15.5	2.3	3.6		17
500	450	12.6	15.3	2.0	4	3.2	18
~300	~395	13	16.5			2.97	19

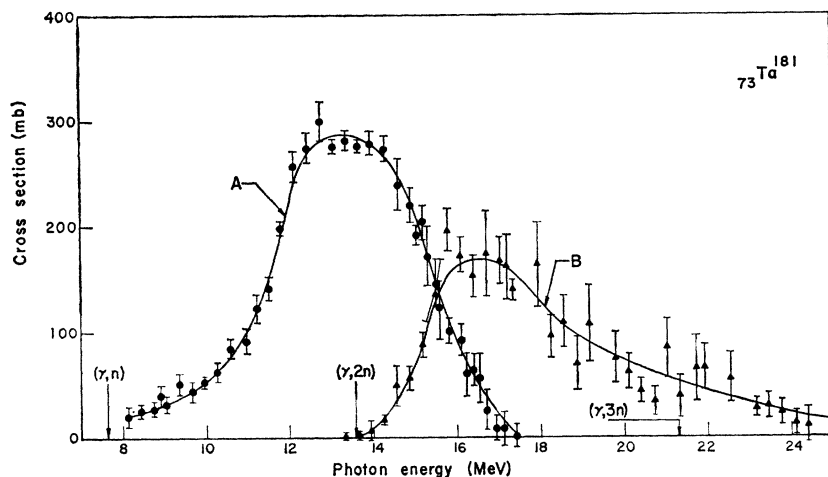


FIG. 2. Partial cross-section curves for Ta. Curve A consists of $\sigma(\gamma,n) + \sigma(\gamma,np)$. Curve B consists of $\sigma(\gamma,2n) + 3\sigma(\gamma,3n)$.

peak cross section of 410 mb at approximately 14.5 MeV, a Γ of 7.5 MeV, and an integrated cross section of 0.079 (NZ/A) or 3.14 MeV-b after correcting for neutron multiplicity by calculation. Later, Fuller and Hayward²⁴ repeated these photoneutron cross-section measurements and obtained two peaks, approximately 383 mb at 12.3 MeV, and 360 mb at 16 MeV. Corrections for neutron multiplicity were again calculated. The integrated cross section deduced for the corrected giant resonance was 1.35 ($0.06 NZ/A$) or 3.22 MeV-b. Lorentz lines were fitted to the giant resonance. From these, the intrinsic quadrupole moment for Ho was found to be 7.6 ± 1.1 b. Welsh and Donahue²¹ measured the total neutron cross section for Ho at several energies using capture gamma rays.

The sample used in the present experiment consisted of 423.6 g of holmium oxide (Ho_2O_3) mounted in a thin-walled plastic container, approximately 4 in. long \times 2-in. diam. The effects of the plastic container and of the

oxygen in the sample were measured in a separate experiment. For the latter, the photoneutrons from an amount of water containing a quantity of oxygen equivalent to that in the sample were measured. The results for Ho are shown in Figs. 4, 5, and 6. The initial neutron data, reduced to cross sections, are shown in Fig. 4. The top and bottom curves were obtained from single and double neutron counting measurements, respectively. It is evident that the total photoneutron measurements give cross sections of 267 and 370 mb at 12.1 and 16.25 MeV, respectively. The lower curve blends with the top curve above 18 MeV, hence the double neutron counting data are not shown above this energy for clarity of presentation. The double neutron data are shown in Fig. 5. The observed threshold for the $(\gamma,2n)$ reaction is 14.8 ± 0.3 MeV, which is considerably below the value 15.90 MeV, given in data tables,²⁵ but is in agreement with the values 14.3 and 14.4 calculated from mass formulas.²⁴

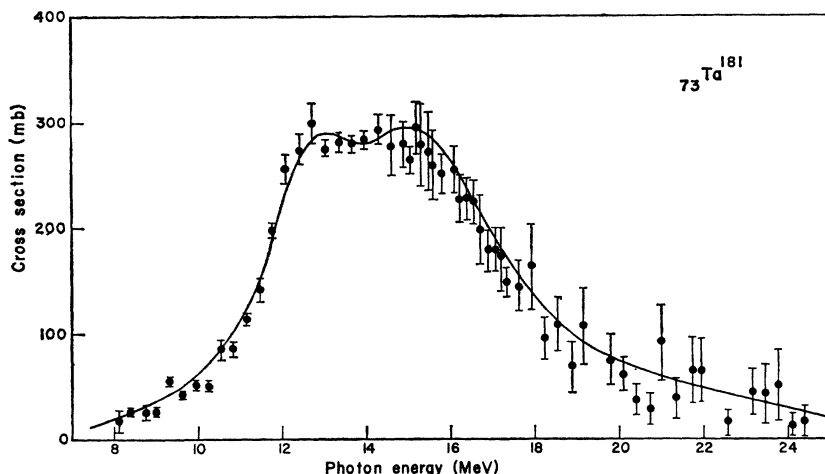
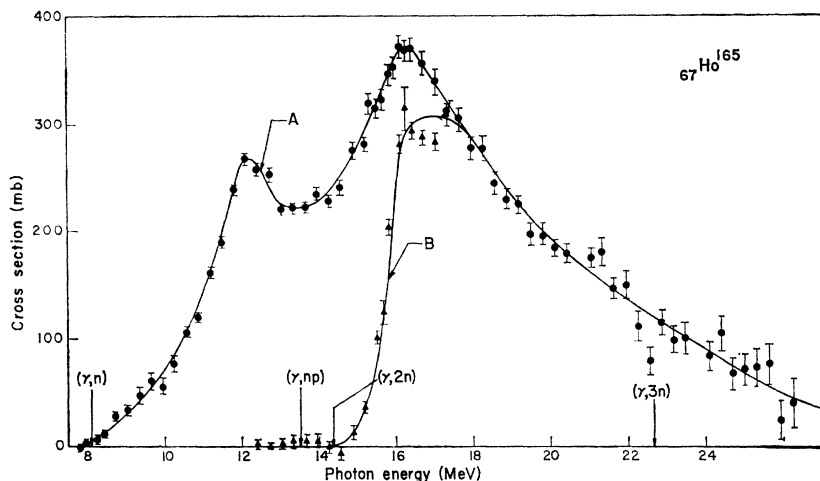


FIG. 3. The formation cross section $\sigma(\gamma,n) + \sigma(\gamma,2n) + \sigma(\gamma,np)$ for the compound nucleus Ta^{181} . The solid curve represents the sum of two Lorentz lines with parameters given in Table III.

²⁴ E. G. Fuller and E. Hayward, Nucl. Phys. **30**, 613 (1962).

²⁵ L. A. Koenig and J. E. Mattauch, in *Nuclear Data Tables*, U. S. Atomic Energy Commission (U. S. Government Printing Office, Washington, D. C., 1960).

FIG. 4. Cross sections for Ho from neutron yield data. Curve A consists of $\sigma(\gamma,n) + 2\sigma(\gamma,2n) + \sigma(\gamma,np) + 3\sigma(\gamma,3n)$ and was obtained from single-neutron counting data. Curve B consists of $2\sigma(\gamma,2n) + 6\sigma(\gamma,3n)$, and was obtained from double-neutron counting data.



The cross-section curves for the (γ,n) and $(\gamma,2n)$ reactions are shown in Fig. 5. The integrated cross sections for $\sigma(\gamma,n)$ and $\sigma(\gamma,2n)$ are 1.47 ± 0.15 and 0.90 ± 0.09 MeV-b, respectively. The data of the giant resonance for the formation cross section of the compound nucleus Ho¹⁶⁵ is shown in Fig. 6. These data were obtained by combining the (γ,n) and $(\gamma,2n)$ data of Fig. 5. Two cross-section peaks, 266 mb at 12.1 MeV and 284 mb at 15.25 MeV, are in evidence. The width of the giant resonance is 6.9 MeV, and the integrated cross section up to 28 MeV is 2.37 ± 0.24 MeV-b. The solid curve in Fig. 6 represents the sum of two Lorentz lines.

ANALYSIS

Lorentz lines were fitted to the formation cross-section data for Ta and Ho. The procedure followed was the same as that which has been discussed in a previous report.⁵ It requires that wing corrections be added to the integrated cross sections, and is designed to reduce

arbitrariness in the choice of parameters characterizing the Lorentz lines. The solid lines in Figs. 3 and 6 each represent the sums of two Lorentz lines which have been fitted to the data for each element. The parameters deduced for these lines are given in Table III. Also given

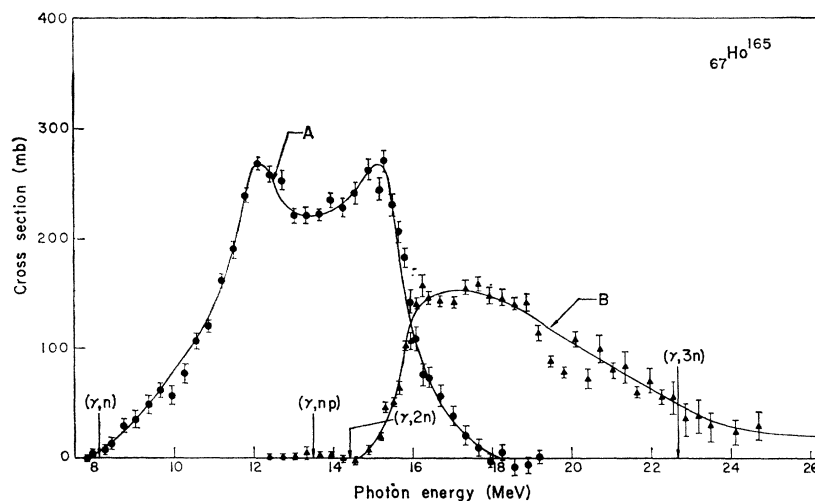
TABLE III. Lorentz line parameters and intrinsic quadrupole moments for Ta and Ho.

Element	σ_a (mb)	Γ_a (MeV)	E_a (MeV)	σ_b (mb)	Γ_b (MeV)	E_b (MeV)	Q_0 (b)
Ta ¹⁸¹	198	3.00	12.75	224	5.0	15.50	6.71 ± 0.74
Ho ¹⁶⁵	200	2.65	12.10	249	4.4	15.75	7.40 ± 0.90

are the intrinsic quadrupole moments, Q_0 , for Ta and Ho which were calculated by use of nuclear radius parameters 1.25 and 1.2 F, respectively.²⁶

From the nuclear formation cross section and the $\sigma(\gamma,2n)$ curves, the ratio of $\sigma(\gamma,2n)$ to the total cross section, $\sigma(\gamma,n) + \sigma(\gamma,2n) + \sigma(\gamma,np)$, was derived as a

FIG. 5. Partial cross-section curves for Ho. Curve A consists of $\sigma(\gamma,n) + \sigma(\gamma,np)$. Curve B contains $\sigma(\gamma,2n) + 3\sigma(\gamma,3n)$.



²⁶ R. Hofstadter, Rev. Mod. Phys. 28, 214 (1956).

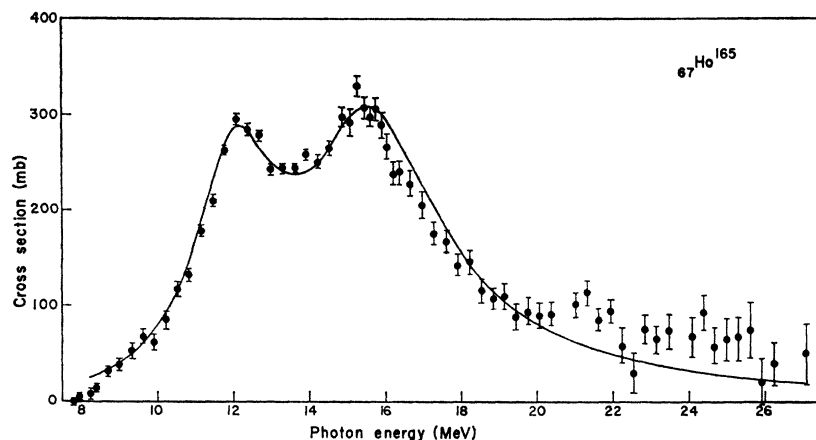


FIG. 6. The formation cross section $\sigma(\gamma, n) + \sigma(\gamma, 2n) + \sigma(\gamma, np)$ for the compound nucleus Ho^{165} . The solid curve represents the sum of two Lorentz lines with parameters given in Table III.

function of energy. An analytic expression for this ratio has been derived by Weisskopf,²⁷ from which it is possible to calculate values for the nuclear level density parameter “ a ” in units of reciprocal MeV. Values for “ a ” deduced by use of this expression are given in the fourth column of Table IV. The procedure followed for calculation of the level density parameters has been discussed in a previous report.⁵ The values deduced for σ_{-2} from the measurements, and those calculated from theory, are given in the second and third columns, respectively, of Table IV. The experimentally determined integrated cross sections up to 28 MeV are given in the fifth column, while the sixth column contains the sum of these experimental integrated cross sections and the wing corrections to the Lorentz lines comprising the nuclear formation cross section. This may be regarded as extending the integration limit to infinite energy. In the last column of Table IV are given theoretical values for the integrated nuclear formation cross sections of Ta and Ho, based upon the dipole sum rule. The integrations extend to infinite energy for the theoretical computations.

Estimated errors in the cross-section measurements and quantities derived from them are approximately $\pm 10\%$.

DISCUSSION AND CONCLUSIONS

The intrinsic quadrupole moment of Ta, from the present measurements, is 6.71 ± 0.74 b, which may be

compared with 6.95 ± 0.27 and 6.7 ± 0.5 deduced from the Coulomb excitation results of McGowan and Stelson²⁸ and Bernstein and Graetzer,²⁹ respectively. For the case of Ho, the intrinsic quadrupole moment of 7.40 ± 0.90 b may be compared with the Coulomb excitation values²⁸ of 8.11 ± 0.5 and 7.56 ± 0.11 . The latter value was obtained by Olesen and Elbeck.³⁰ Agreement of the results of the present measurements with those obtained from Coulomb excitation is evident. The quadrupole moments were deduced from the mean energies for two Lorentz lines fitted to the giant resonances. It has been suggested by Inopin³¹ that the giant resonance might be resolvable into three Lorentz lines having equal areas, which would characterize a triaxial or ellipsoidal nucleus. Attempts were made to obtain such a fit, using a systematic approach similar to that previously outlined.⁵ It was not found possible to fit three Lorentz lines to the data of either Ho or Ta, hence it was concluded that these nuclei are essentially spheroidal.

A comparison of the experimental values of σ_{-2} with theory can be obtained from the second and third columns of Table IV. Good agreement can be seen for Ho, but the Ta value falls slightly below the calculated value. The level density parameters deduced for these elements may be compared with those obtained by other experimental methods. For Ta the value 15.7 ± 0.8 reciprocal MeV obtained in the present experiment falls in the range of those obtained from (n, n') experiments,³²

TABLE IV. Integrated cross sections, level density parameters, and σ_{-2} values.

Element	σ_{-2} (mb/MeV)	$0.00225A^{5/3}$ (mb/MeV)	a (MeV ⁻¹)	$\int_{\sigma}^{28} \sigma dE$ (MeV·b)	$\int_{\sigma}^{28} \sigma dE + W$ (MeV·b)	$0.06 NZ/A$ (MeV·b)
Ta ¹⁸¹	10.88	13.03	15.7	2.24	2.59	2.61
Ho ¹⁶⁵	10.93	11.17	22.0	2.37	2.68	2.38

²⁷ J. M. Blatt and V. F. Weisskopf, *Theoretical Nuclear Physics* (John Wiley & Sons, Inc., New York, 1952), Chap. 8.

²⁸ F. K. McGowan and P. H. Stelson, *Phys. Rev.* **109**, 901 (1958).

²⁹ E. M. Bernstein and R. Graetzer, *Phys. Rev.* **119**, 1321 (1960).

³⁰ M. C. Olesen and B. Elbeck, *Nucl. Phys.* **15**, 134 (1960).

³¹ E. V. Inopin, *Zh. Eksperim. i Teor. Fiz.* **38**, 992 (1960) [translation: *Soviet Phys.—JETP* **11**, 714 (1960)].

³² D. B. Thompson, Doctoral thesis, University of Kansas, 1960, (unpublished).

which have values from 28.8 to 13 reciprocal MeV. For Ho, the value 22.0 ± 1.1 reciprocal MeV is in the same range as those for elements in the same region of the periodic table.^{32,33}

The integrated cross sections shown in the fifth column of Table IV were obtained from the experimental data, up to a maximum energy of 28 MeV. When the component Lorentz curves had been determined, corrections for the energy region between 28 MeV and infinite energy (i.e., the wing corrections) were calculated and added to the original values. No correction has been made for the contribution of (γ, p) reactions since it is negligible.³⁴ The corrected values for the integrated cross sections are given in the sixth column. The wing corrections account for 11.5 and 13% of the total integrated cross section for Ho and Ta, respectively. If the Lorentz lines are a true representation of the components of the giant resonance, then the values listed in the sixth column should be used for comparison with theoretical values determined from the dipole sum rule, since both represent integrations to infinite energy. It can be seen from the sixth and seventh columns of Table IV that the corrected experimental value agrees well with the sum rule for Ta, but is about 12.5% too high for the case of Ho. This is only slightly greater than the estimated error for the integrated cross section, hence cannot be considered as highly significant.

In summary, the splittings in the giant resonances of Ta and Ho which were observed by other investigators have been confirmed in the present experiment for which essentially monochromatic photons have been employed and contributions from higher multiplicity reactions have been measured. Lorentz line components for the

giant resonances of Ta and Ho were determined by taking into account the measured areas of the cross-section curves and utilizing a method designed to reduce the arbitrariness in choice of parameters. With these techniques, pronounced splitting in the giant resonances of these elements was observed, which yielded values for intrinsic quadrupole moments in agreement with those determined from Coulomb excitation measurements. Level density parameters were experimentally determined. The experimental value of σ_{-2} for Ho agreed with the theoretical one, but that for Ta was about 15% lower. Values for the integrated cross sections, with added wing corrections, agreed with those determined from the sum rule calculations, with no account being taken of exchange forces. Cross-section values determined in the present measurements agree fairly well with those previously obtained by use of monochromatic photons. No evidence of triple splitting of the giant resonances for Ho or Ta was found, hence it was concluded that these nuclei are essentially spheroidal. Measurements of the number of annihilation photons by use of a gamma-ray spectrometer agreed within 3% with those calculated from measurements of the number of positrons.

ACKNOWLEDGMENTS

The authors wish to acknowledge assistance with measurements and analysis of the early data on Ta given by C. P. Jupiter, N. A. Kerr, and N. E. Hansen. They also wish to thank Dr. C. D. Bowman for help with measurements, and to acknowledge the cooperation of the Accelerator operating and maintenance personnel.

This work was performed under the auspices of the U. S. Atomic Energy Commission.

³² E. Erba, U. Facchini, and E. Saetta Menichella, *Nuovo Cimento* **22**, 1237 (1961).

³⁴ M. Elaine Toms and W. E. Stephens, *Phys. Rev.* **98**, 626 (1955).